Topological Phase Transition Properties of Interacting Bose-Einstein Condensates in Quasi-Periodic Potential Wells

Jianrong Wen
School of Microelectronics, Shanxi University of Electronic Science and Technology, Linfen 041000, Shanxi, China
Corresponding author: Jianrong Wen (e-mail: sxdz1219888@163.com)

ABSTRACT Topological state characterization in interacting quasi-periodic systems remains challenging because conventional band-topology approaches become invalid in the presence of strong many-body correlations and broken translational symmetry. This study develops a generalized many-body Zak phase framework for investigating topological phase transitions in Bose–Einstein condensates confined within quasi-periodic potential wells. By introducing a quasimomentum manifold derived from quasi-periodic phase symmetry and constructing gauge-continuous ground-state families, topological invariants are directly extracted from many-body wavefunctions without relying on Bloch bands, Brillouin zones, or bulk energy gaps. The proposed approach is integrated with density matrix renormalization group calculations to establish a unified characterization of superfluid, localized, and critical regimes. Results show that a stable topologically nontrivial phase emerges at $U/J = 3.2$ and $\Delta/J = 2.8$, where the momentum distribution exhibits symmetric peaks at $k = \pm\pi/2$ with an amplitude of 1.87. Open-boundary analysis reveals strongly localized edge modes with approximately 90% density concentration near system boundaries, while the entanglement spectrum displays a symmetry-protected doubly degenerate structure. The results demonstrate that interaction and quasi-periodicity jointly stabilize nontrivial topological states and associated wave-localization phenomena. The proposed framework provides a rigorous methodology for analyzing topological phase evolution, geometric-phase transitions, and wave propagation characteristics in strongly correlated quasi-periodic systems.

INDEX TERMS topological phase transition, many-body Zak phase, quasi-periodic structures, wave localization

I. INTRODUCTION

THE study of topological quantum states has profoundly changed the understanding of quantum phases and phase transitions in recent years. Its core lies in characterizing the nontrivial quantum order of matter through global topological invariants. Bose-Einstein condensates, as highly controllable macroscopic quantum systems, have been widely used in cold atom experiments to simulate phenomena such as topological bands, artificial gauge fields, and boundary states [1,2]. Introducing quasi-periodic potentials into this system not only expands the symmetry framework of traditional periodic lattices but also provides a new platform for exploring critical topological phases between order and disorder [3,4]. By systematically studying interaction-induced topological phase transitions, this work advances non-periodic topology theory and the understanding of geometric quantum effects in strongly correlated systems, providing theoretical foundations for achieving robust quantum states.

The topological classification of interacting Bose systems in quasi periodic potentials faces multiple theoretical obstacles. The topological invariants in single particle images depend on the Bloch band structure and gap protection, while the quasi-periodic potential itself lacks exact translational symmetry, which prevents the direct application of the standard Bloch band theory and the associated Brillouin zone construction based on perfect periodicity [5,6]; At the same time, the interaction of s-waves between atoms introduces nonlinearity and multi-body correlation, making the ground state no longer reducible to a single particle occupied state, and the traditional band topology description completely collapses [7,8]. More complicated is that the system can simultaneously undergo superfluidization localization transition, spectral criticality, and topological structure evolution under parameter control, and the coupling of the three makes it difficult to identify phase boundaries through local order parameters [9,10]. In addition, although the cold atom experiment can accurately achieve the quasi periodic potential of the bichromatic lattice structure and adjust the Feshbach resonance control interaction, it lacks observable measurements directly corresponding to the multi-body topological order, which restricts the experimental verification of theoretical predictions [11].

Preliminary progress has been made in research under non interacting or weak interacting limits. The Aubry-André model, a quasi-periodic tight-binding model, reveals localized phase transitions. Recent studies have extended this model to systems with artificial spin-orbit coupling, successfully predicting the existence of edge states through single-particle Zak phases [12,13]. In recent years, some studies have attempted to combine the Gross–Pitaevskii mean-field equations with topological band structures to analyze the influence of weak nonlinearity on edge mode stability. However, this method ignores quantum fluctuations and fails in the strong interaction region [14,15]. Another type of work is based on the Bose–Hubbard model, using DMRG or quantum Monte Carlo to calculate the ground state and indirectly inferring topological order through entanglement spectrum degeneracy. However, such criteria rely on symmetry protection and cannot provide quantitative topological invariants [16,17]. Some studies have attempted to define Berry phase based on multi-body wave functions, but it is difficult to construct a gauge continuous parameter path under non periodic boundary conditions, resulting in non unique phase definitions [18,19]. These methods are either limited by weak correlation assumptions, lack strict topological invariants, or cannot establish direct connections with observable quantities in real space, and have not yet solved the universal classification problem of topological phases in quasi periodic BEC (Bose-Einstein condensate) interactions.

To solve the problem of the lack of strict and computable topological invariants in quasi periodic systems under multi-body effects, this paper constructs a generalized Zak phase theory based on the multi-body ground state phase structure. By identifying the implicit quasi translational symmetry in quasi periodic potentials, this paper defines continuous quasi momentum parameters and maps the ground state of finite systems to a family of functions of k through gauge continuous extension; Constructing projection operators on this parameter manifold, this paper further defines the geometric phase in path integral form, which maintains gauge invariance and topological robustness in the presence of interactions. This method does not rely on band-derived concepts such as Brillouin zones or periodic boundary conditions, nor does it require a bulk energy gap, and is directly derived from the multi-body ground state wave function. Combined with high-precision numerical techniques such as DMRG, this framework quantitatively characterizes topological phase transitions in superfluidity, localization, and critical regions, providing a clear theoretical basis for interpreting experimental time-of-flight imaging.

II. CONSTRUCTION AND CALCULATION METHOD OF MULTI-BODY TOPOLOGICAL INVARIANTS

To clarify the theoretical framework and technical path for calculating the multi-body topological invariants of quasi periodic Bose systems in this article, Figure 1 shows the computationa l framework.

Figure 1 presents the complete chain from microscopic models to topological criteria in a modular manner: the "Physical Model Construction" module establishes a one-dimensional open boundary quasi periodic Bose-Hubbard Hamiltonian; The "Multi-body Ground State and Quasi Momentum Manifold Construction" module serves as the core area. By introducing the potential field phase as the continuous parameter κ, a Hamiltonian family is constructed and a gauge continuous ground state extension is achieved, breaking through the traditional Bloch periodicity limitation; The "Multi-body Topology Invariant Extraction" module defines a many-body Zak phase that does not rely on band structures. It obtains strict topological order parameters through geometric phase integration and directly correlates phase diagrams, edge states, and experimental observables. The overall architecture embodies the three-layer logic of "model, manifold, and invariant", highlighting the theoretical consistency and computational feasibility of topological classification methods in quasi periodic multi-body systems.

A. CONSTRUCTION OF HAMILTONIAN FOR QUASI PERIODIC BOSE-HUBBARD MODEL

The physical system studied in this article is described by a quasi periodic Bose-Hubbard model on a one-dimensional open boundary chain [20,21], with its Hamiltonian written as:

$$\begin{aligned}\hat{H} = & -J\sum_{j=1}^{L-1}\left(\hat{a}_j^{\dagger}\hat{a}_{j+1}+H.c.\right)\\ & +\frac{U}{2}\sum_{j=1}^{L}\hat{n}_j\left(\hat{n}_j-1\right)\\ & +\Delta\sum_{j=1}^{L}\cos\left(2\pi\beta j+\phi\right)\hat{n}_j\end{aligned} \tag{1}$$

In Formula 1, $\hat{a}_j^{\dagger}$ and $\hat{a}_j$ are the boson generation and annihilation operators at the jth lattice point, $\hat{n}_j=\hat{a}_j^{\dagger}\hat{a}_j$ is the particle number operator, and L is the total number of lattice points. The first item describes the quantum tunneling process between nearest neighboring lattice points, where $J>0$ represents the tunneling strength and is set in energy units; The second term characterizes the local s-wave repulsion interaction, where U is the strength of the interaction, and its polarity determines repulsion or attraction. This study only considers the repulsion case where $U\geq 0$. The third term is the external quasi periodic potential, where Δ is the modulation depth and controls the potential barrier strength, β is the modulation frequency, taken as an irrational number (usually using the golden ratio conjugate $\beta=(\sqrt{5}-1)/2$ to avoid periodic approximation), and $\phi\in[0,2\pi)$ is the global

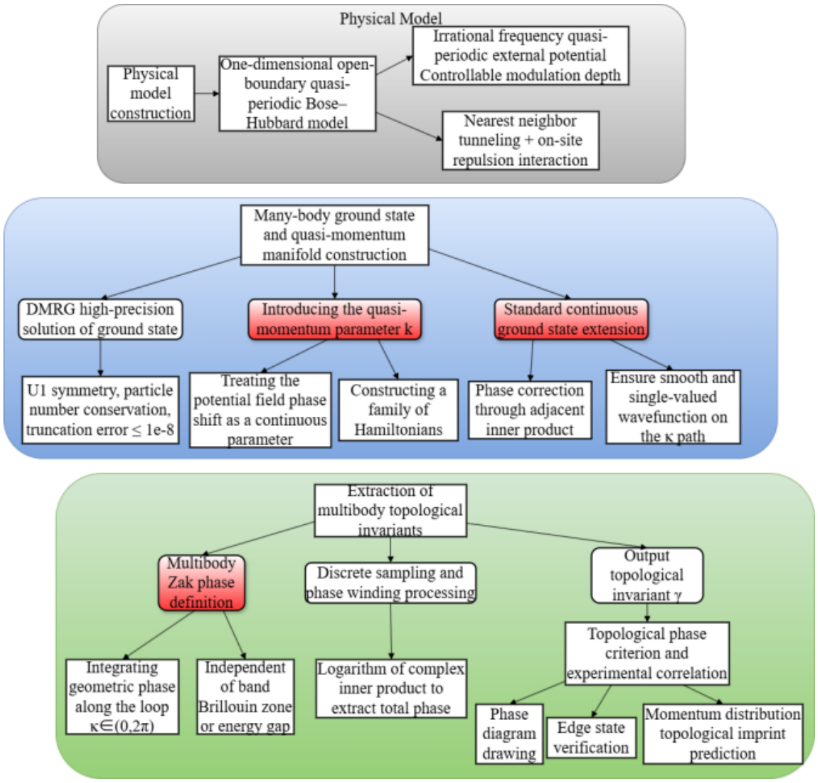

FIGURE 1. Computational framework for multi-body topological invariants of quasi periodic Bose systems with interactions

phase shift, used as a continuous parameter to construct the quasi momentum manifold. The system adopts open boundary conditions to clearly distinguish between body and boundary states. The total number of particles N is fixed, and the number of fillers is set as a unit (N=L) to ensure significant competition between Mott physics and superfluidity in this parameter region. This Hamiltonian fully characterizes the multi-body quantum dynamics of the coupling of tunneling, interaction, and non periodic external potential experienced by Bose gases in a bichromatic lattice during cold atom experiments, providing a microscopic basis for the subsequent definition of multi-body topological invariants.

B. HIGH PRECISION NUMERICAL SOLUTION OF MULTI-BODY GROUND STATE

The multi-body ground state is solved with high accuracy using the DMRG method under fixed total particle number N=L and open boundary conditions [22,23]. The system wave function is expanded under the Matrix Product State (MPS) representation, and its canonical form satisfies left orthogonal and right orthogonal constraints to ensure the stability of variational optimization.

During the iteration process of DMRG, a dual lattice update strategy is adopted to perform Lanczos diagonalization on the effective Hamiltonian [24,25]. The energy convergence criterion is set to ensure that the relative change in ground state energy between adjacent iteration steps is less than 10^{-10}, while limiting the truncation error of MPS to no more than 10^{-8}, ensuring that quantum correlations are fully preserved. To avoid the local minimum trap, the initial MPS adopts a uniformly filled state of random small perturbation superposition, and the uniqueness of the results is verified through multiple independent runs. The maximum number of reserved states in the calculation is set to 2000, which is sufficient to cover the entire parameter region from weak interaction superfluid phase to strong interaction localized phase, and to maintain the feasibility of memory and computation time when the system size is less than or equal to 80. All calculations are based on the U(1) symmetric quantum block structure with strict particle number conservation, effectively improving efficiency and ensuring the physical correctness of the ground state. The key numerical parameter configuration includes the number of grid points, range of interaction strength, quasi periodic modulation depth, truncation error threshold, and MPS reserved state number, as shown in Table 1.

TABLE 1. DMRG Calculation Parameter Settings

Parameter	Symbolic representation	Range of values or fixed values	Explanation
Number of grid points	L	30, 40, 60, 80	Open boundary chain length, used for finite-size scaling analysis
Total number of particles	N	N=L	Unit fill conditions
Filling factor (ρ = N/L)	ρ	1 (fixed)	The system is studied at unit filling (ρ=1) to focus on the competition between interaction and quasi-periodicity under maximal commensurate density.
Tunneling strength (unit of energy)	J	1.0	Energy and length scale benchmarks
Interaction strength	U	0.0 – 6.0	Covering weak, medium and strong repulsion areas
Quasi-periodic modulation depth	Δ/J	0.0 – 4.0	Controlling the quasi-periodic potential intensity
Modulation frequency	β	($\sqrt{5}$-1)/2	Golden ratio conjugation ensures irrational modulation.
Upper limit of truncation error	—	1×10^{-8}	Controlling MPS approximate accuracy
Maximum number of retained states	—	2000	Guarantee convergence of strongly correlated regions
Energy convergence threshold	—	1×10^{-10}	Criterion for relative change in ground state energy

Table 1 lists the complete parameter configurations used in DMRG calculations, covering both physical scale and numerical control levels. The number of grid points covers 30 to 80, which is used for subsequent finite size scaling analysis to eliminate boundary effect interference. The range of values for interaction strength and quasi periodic modulation depth covers the superfluid, critical, and localized regions respectively, ensuring that the topological phase transition points can be fully captured. The modulation frequency is fixed to an irrational number and strictly maintains quasi periodicity. At the algorithmic level, the upper bound of truncation error, maximum number of retained states, and energy convergence threshold work together to ensure high fidelity reconstruction of multi-body wave functions under strongly correlated regimes. This parameter system strikes a balance between computational accuracy and resource consumption, laying a numerical foundation for the reliable extraction of multi-body topological invariants.

C. CONSTRUCTION OF QUASI MOMENTUM MANIFOLDS AND EXTENSION OF GROUND STATE FAMILIES

The construction of quasi momentum manifolds is based on the implicit continuous phase symmetry in quasi periodic potentials. The quasi periodic potential term in the original Hamiltonian contains a global phase shift ϕ, which is physically unobservable but can be used as a mathematical continuous variable to construct a parameter space. The global phase shift ϕ can be regarded as a continuous parameter $\kappa \in [0, 2\pi)$, thus constructing a family of Hamiltonian $\hat{H}(\kappa)$ that satisfies $\hat{H}(\kappa + 2\pi) = \hat{H}(\kappa)$, where k plays the role of a Bloch like quasi momentum. Although the system lacks true translational symmetry, $\hat{H}(\kappa)$ is strictly periodic at $\kappa \to \kappa+2\pi$, forming a compact one-dimensional parameter loop.

For each discrete sampling point, $\kappa_n = 2\pi n/N$ (n=0, 1,..., N-1, N is the number of samples), the corresponding ground state $|\Psi_0(\kappa_n)\rangle$ is solved using DMRG to form a parameterized multi-body ground state family. To ensure the normative continuity of subsequent geometric phase calculations, it is necessary to perform normative corrections on the original ground state sequence: starting from κ_0, adjust the overall phase factor between adjacent points in sequence, so that the inner product $\langle\Psi_0(\kappa_n)|\Psi_0(\kappa_{n+1})\rangle$ is a positive real number. This process is implemented through a recursive relationship:

$$|\tilde{\Psi}_0(\kappa_{n+1})\rangle = \frac{\langle\tilde{\Psi}_0(\kappa_n)|\Psi_0(\kappa_{n+1})\rangle^*}{|\langle\tilde{\Psi}_0(\kappa_n)|\Psi_0(\kappa_{n+1})\rangle|}|\Psi_0(\kappa_{n+1})\rangle \tag{2}$$

In Formula 2, $|\tilde{\Psi}_0(\kappa_0)\rangle = |\Psi_0(\kappa_0)\rangle$. The extension of this specification ensures that the ground state family is gauge-smooth and single valued on the k-ring, providing a mathematical basis for the definition of manybody Zak phases. The number of sampling points N=200 has been verified to be sufficient to converge the phase integral to within 10^{-3} radians, and the dependence of the results on N and L has been excluded through finite size analysis. This construction does not rely on real lattice periodicity and only utilizes the phase shift invariance of quasi periodic potentials, making it suitable for multi-body systems with coexisting open boundaries and interactions.

D. NORM INVARIANT DEFINITION AND NUMERICAL INTEGRATION OF MANY-BODY ZAK PHASE

The many-body Zak phase is defined as the geometric phase of the ground state group $|\tilde{\Psi}_0(\kappa)\rangle$ along the parameter ring $\kappa \in [0, 2\pi)$, expressed as:

$$\gamma = \mathrm{Im}\int_0^{2\pi}\langle\tilde{\Psi}_0(\kappa)|\partial_\kappa\tilde{\Psi}_0(\kappa)\rangle\, d\kappa \tag{3}$$

$|\tilde{\Psi}_0(\kappa)\rangle$ is the multi-body ground state after gauge continuous extension, satisfying the periodic boundary condition $|\tilde{\Psi}_0(2\pi)\rangle = e^{i\theta}|\tilde{\Psi}_0(0)\rangle$, and the overall phase θ does not affect the physical value of γ. This phase only depends on the intrinsic geometric structure of the ground state manifold, remains invariant to local gauge transformations, and is a topological invariant in the connected region where the Hamiltonian energy gap of the system is not closed. In numerical implementation, k is discretized into N equidistant points $\kappa_n = 2\pi n/N$ (n=0, 1,..., N-1), and the derivative term is approximated by finite difference and integrated into a sum form:

$$\gamma \approx \mathrm{Im} \sum_{n=0}^{N-2} \langle \tilde{\Psi}_0(\kappa_n)|\tilde{\Psi}_0(\kappa_{n+1})\rangle + \mathrm{Im}\langle \tilde{\Psi}_0(\kappa_{N-1})|\tilde{\Psi}_0(\kappa_0)\rangle \tag{4}$$

The last item is to ensure that the loop is closed. Due to the fact that all adjacent inner products are positive real numbers after standard correction, their phase is zero, the accumulated global phase is extracted via phase unwinding (gauge fixing) in the numerical implementation of the complex logarithm, yielding a nonzero γ. This phase unwinding procedure is equivalent to fixing a smooth gauge along the parameter loop and ensures the extracted Zak phase is consistent with the topological invariant defined in the continuum limit. The actual calculation uses:

$$\gamma = -\,\mathrm{Im}\ln \prod_{n=0}^{N-1} \langle \tilde{\Psi}_0(\kappa_n)|\tilde{\Psi}_0(\kappa_{n+1})\rangle \tag{5}$$

$\kappa_N \equiv \kappa_0$, this form automatically handles phase entanglement and avoids the accumulation of numerical errors. The number of samples varies by less than 0.01π between L=60 and L=80, indicating that the results are not dominated by finite size. This definition does not depend on single-particle band structures, Brillouin zones, or bulk gaps, and is applicable to quasi-periodic many-body systems where interactions lead to continuous or critical energy spectra, providing a rigorous and computable criterion for topological phases.

III. EXPERIMENTAL DETECTION AND VERIFICATION OF OBSERVABLE TOPOLOGICAL PHASE TRANSITION PROPERTIES

A. COLD ATOM SYSTEM PARAMETER CONFIGURATION

The theoretical model of this study can be directly mapped to the experimental realization of ultracold Bose atoms in an optical lattice. The system uses ^{87}Rb atoms as the working medium, and their ground-state hyperfine level as the internal state of the condensed-state atoms. The one-dimensional quasi-periodic optical lattice is formed by the superposition of two collinear, counter-propagating laser fields. The wavelength of the primary lattice is $\lambda_1 = 1064$ nm, and the wavelength of the secondary modulation lattice is $\lambda_2 = 532$ nm, with a wavelength ratio of 2:1, ensuring that the spatial frequency of the modulation term is an irrational multiple (corresponding to $\beta = (\sqrt{5}-1)/2$ in the theoretical model). The primary lattice depth V_1 controls the nearest-neighbor tunneling intensity J, and the secondary lattice depth V_2 determines the quasi-periodic potential modulation depth Δ. Both are independently adjustable by the laser power. The s-wave scattering length a_s is tuned using a wide Feshbach resonance [26], thereby setting the interaction strength U, whose ratio U/J is determined by a_s, atomic mass, lattice depth and transverse trapping frequency. The system uses a strong harmonic oscillator potential to achieve quasi-one-dimensional confinement in the transverse direction, and the number of axial lattice points is controlled between 30 and 80 by the size of the Gaussian spot of the main lattice beam. The total number of atoms is precisely set to N=L by the initial magneto-optical trap loading rate and the evaporation cooling endpoint. There is a clear quantitative mapping relationship between the key parameters in the theoretical model and the adjustable physical quantities in the cold atom experiment.

B. EXPERIMENTAL DETECTION SCHEMES FOR TOPOLOGICAL OBSERVABLES

Experimental verification of topological phases depends on converting abstract multi-body topological invariants into measurable physical signals. Time-flying absorption imaging is used to obtain momentum distribution n(k), and by releasing the atomic cloud and recording the density distribution after free expansion, the coherent structure of the system in the lattice momentum space is inverted; in-situ high-resolution imaging (such as quantum gas microscopy) directly measures the local density $\langle \hat{n}_j \rangle$ in real space, which is used to identify the boundary localization mode and its occupancy rate [27]; the two-point density correlation function $g^{(2)}(j,j') = \langle \hat{n}_j \hat{n}_{j'} \rangle - \langle \hat{n}_j \rangle \langle \hat{n}_{j'} \rangle$ is statistically reconstructed through repeated experiments, and its low-frequency mode can approximately reflect the topological degeneracy characteristics of the entanglement spectrum [28]. Furthermore, quantum quenching dynamics is used as a dynamic probe: the system is abruptly switched from a topological initial state to a non-topological potential, and the survival time of boundary excitations is monitored; its long lifetime behavior corresponds to topological protection [29]. There is a clear one-to-one correspondence between the above observables and theoretical topological criteria, as shown in Table 2.

TABLE 2. Mapping relationship between topological observables and theoretical signals

Theoretical topological indicator	Experimental observable	Topological signal signature
Many-body Zak phase $\gamma=\pi$	Momentum distribution n(k)	Sharp asymmetric peaks at k=$\pm\pi$/2, distinct from the trivial-phase central peak at k=0
High edge-mode occupation	In-situ local density $\langle \hat{n}_j \rangle$	Significantly enhanced density at boundary sites; edge occupation> 85%
Twofold degeneracy in entangle- ment spectrum	Noise correlation spectrum (low-frequency modes)	Symmetric double-peak structure in density–density correlations, with peak positions locked by topologi- cal phase
Topological phase transition point	Coherence decay rate of edge modes after quantum quench	Longest coherence lifetime at the transition point, exhibiting a maximum in survival time

Table 2 establishes a direct bridge from multi-body topology theory to cold atom experimental detection. The quantitative threshold (edge occupation > 85%) is obtained for the specific system size L=60 and modulation depth Δ/J=2.8 studied herein, and may vary with system size and parameters. The characteristic peak position of momentum distribution is determined by the many-body Zak phase and does not depend on the existence of edge states, making it suitable for periodic boundaries or high loss systems; The local density profile provides the most intuitive topological evidence in real space and is robust to interactions; Although noise correlation is an approximate method, it can still be used as an indirect criterion for entanglement topological order in the absence of full quantum state tomography conditions; Quenching kinetics provides a time-domain criterion to avoid extreme dependence on the accuracy of ground state preparation. The four types of signals complement each other and together form a multidimensional experimental verification system for aligned periodic interaction BEC topological phases.

C. TOPOLOGICAL PHASE TRANSITION CHARACTERISTICS AND MULTIDIMENSIONAL INDEX VERIFICATION

To reveal the topological phase transition characteristics of interacting Bose Einstein condensates in quasi periodic potential wells, this section analyzes them from four complementary dimensions. This article establishes the topological phase boundary (order parameter dimension) through the abrupt behavior of manybody Zak phases; Secondly, this article examines the stability and local characteristics (edge excitation dimension) of edge excited modes in open boundary systems. It analyzes the characteristic peak positions (momentum space imprint dimension) corresponding to topological non mediocrity in momentum distribution; Finally, this article verifies the quantum correlation characteristics (quantum entanglement dimension) of multibody topological order from the degenerate structure of entanglement spectra. The above multidimensional indicators mutually confirm and together constitute a systematic characterization of the topological phase transition of the system.

1) Abrupt Transitions in Many-Body Zak Phases and Determination of Topological Phase Boundaries

To accurately identify the topological phase boundaries of interacting Bose-Einstein condensates in quasiperiodic potentials, this section uses high-precision DMRG calculations to determine the evolution behavior of the many-body Zak phases under a wide range of interaction intensities and quasi-periodic modulation depths, systematically plotting their topological phase diagrams to determine the critical parameter regions for phase transitions. As a strictly multibody topological invariant, the abrupt changes in this phase directly indicate alterations in the topological order of the bodies, as shown in Figure 2.

Figure 2 shows the distribution of the normalized many-body Zak phase γ/π on the U/J–Δ/J parameter plane. The horizontal axis represents the quasi-periodic modulation depth Δ/J, and the vertical axis represents the interaction strength U/J. The non-interacting Aubry–André model does not support the topological phase, and its many-body Zak phase is zero. At U/J=3.2, the many-body Zak phase γ/π rapidly jumps to 1 with increasing quasi-periodic modulation depth. The phase transition point (defined as γ/π=0.5) is located at Δ/J≈1.0, reaches 0.93 at Δ/J=1.2, and tends to saturate to 1.0 at Δ/J=1.6. When Δ/J = 2.8, the system is in a stable topologically nontrivial phase with γ/π = 1.0, indicating that the multi-body topological order has been fully established. This shift originates from the repulsive interaction effectively enhancing the local barrier through the Hartree potential, equivalently increasing the quasi-periodic modulation intensity, thereby triggering spectral topological reconstruction at a higher Δ/J. Simultaneously, the interaction suppresses manybody quantum fluctuations, causing the phase coherence of the ground-state wavefunction to form a stable entanglement in the parameter space, resulting in γ/π approaching the ideal quantization value. The phase boundary shifts to the left with increasing U/J, reflecting the renormalization effect of many-body correlation on the critical localization threshold. The results indicate that the existence of the topological phase essentially depends on interaction-induced many-body band topology, rather than a single-particle mechanism.

2) Stability and Spatial Localization Characteristics of Edge States

To verify the body edge correspondence of the topological phase of interacting Bose Einstein condensates in quasi periodic potentials, the low-energy excitation spectra of an open boundary system with precise diagonalization were studied, and the real space density distribution of the excited states was calculated to confirm the existence, energy positions, and local properties of boundary modes. This analysis

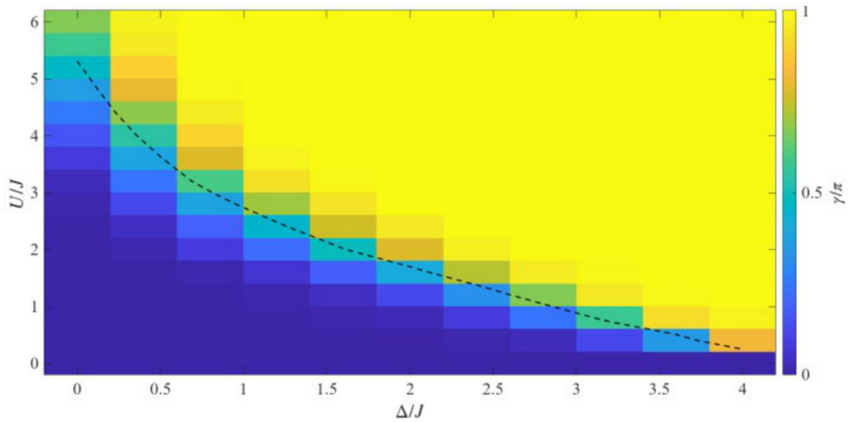

FIGURE 2. Phase diagram of many-body Zak phase as a function of interaction and modulation depth

directly tests whether the topological order predicted by the many-body Zak phase behaves as protected edge excitations in real space, and the results are shown in Figure 3.

Figure 3 (a) shows the excited state numbers on the horizontal axis and the excited energy (in J) on the vertical axis. The data shows that the energies of excited states 2 and 3 are 0.0021J and 0.0023J, respectively, which are significantly lower than the fourth excited state (0.187J), forming an energy gap of approximately 0.18J; In Figure 3 (b), the horizontal axis represents the grid point positions j from 1 to 60, and the vertical axis represents the local density. The edge modes reach 0.872 at j=1 and j=59, respectively, and decay exponentially towards the interior. The sum of density weights within the five grid points on the edge accounts for nearly 90% of the total weight of the excited state density distribution, indicating that the excited state is highly localized at the system boundary. The low edge excitation energy is due to the zero energy mode induced by topologically non trivial states under open boundary conditions, and the interaction suppresses the quantum fluctuations of the states, preventing edge excitation from hybridization and maintaining its near zero energy characteristics; High locality is caused by the multi-body localization effect induced by quasi periodic potentials under strong interactions, which forms bound states at the boundary due to potential field truncation.

3) Identification of Topological Signals in Momentum Distribution

To establish a direct connection between multi-body topological order and experimental observables, based on the principle of time-of-flight imaging, the momentum distribution n(k) of the system under topological non trivial and trivial phases is calculated to identify the momentum space topological imprint determined by the many-body Zak phase. This analysis transforms abstract geometric phases into momentum spectral features that can be directly measured in cold atom experiments, as shown in Figure 4.

The horizontal axis of Figure 4 represents the lattice momentum k, plotted over the conventional interval [-π, π] (corresponding to the reciprocal lattice spacing of the underlying primary optical lattice) for ease of comparison with periodic systems. It is important to note that in our quasi-periodic system, this interval does not represent a true Brillouin zone due to the broken discrete translational symmetry; it is used here as a conventional momentum-space reference frame. And the vertical axis represents the normalized momentum distribution n(k). In the topologically nontrivial phase (Δ/J=2.8), n(k) exhibits a symmetrical sharp peak at k=$\pm\pi/2$, reaching a height of 1.87; while in the topologically trivial phase (Δ/J=1.2), the main peak is located at k=0, with a peak value of 2.15. This peak shift originates from the global phase entanglement of the manybody ground-state wavefunction on the quasi-momentum manifold: when the many-body Zak phase γ=π, the wavefunction has an alternating sign structure in real space, and its Fourier transform necessarily strengthens at k=$\pm\pi/2$; while when γ=0, the wavefunction has a uniform sign, and the momentum weights are concentrated at k=0. This interaction maintains this phase coherence, making the topological signal significant even in strongly correlated regions. The results show that the peak position of the momentum distribution can serve as a volume topology criterion without boundary probing.

4) Multi-body Topology Verification of Entangled Spectra

To verify the nonlocality of topological order from the perspective of many-body quantum correlation, this experiment divides the system into half-chains and calculates the eigenspectrum (i.e., entanglement spectrum) of the reduced density matrix to detect the topological degeneracy protected by symmetry. This method does not rely on boundary conditions or bandgap assumptions and directly reflects the global topological properties of the ground state wavefunction. The results are shown in Figure 5.

The horizontal axis of Figure 5 represents the entanglement level number denoted by α, and the vertical axis represents the entanglement spectrum, where λ_α is the eigenvalue of the reduced density matrix. In the topologically nontrivial phase (Δ/J=2.8), the first two energy levels are 0.321 and

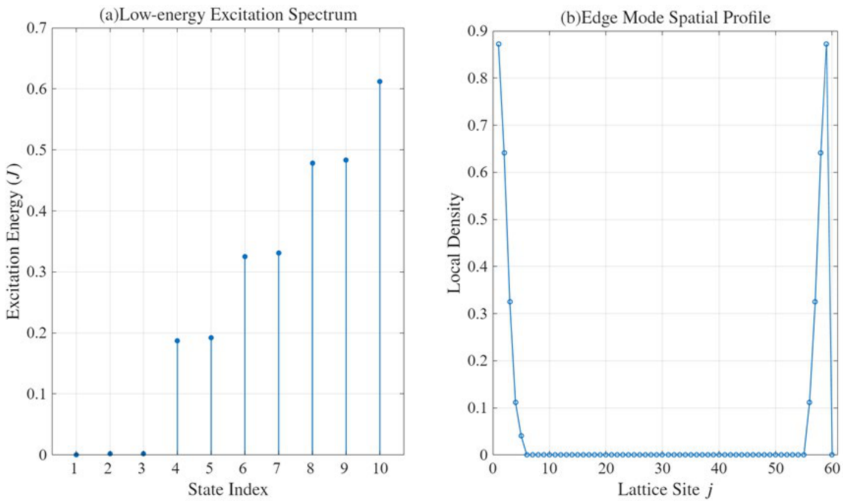

FIGURE 3. Low energy excitation spectrum and edge state spatial distribution of an open boundary system (a) Low energy excitation spectrum (b) Edge mode spatial contour

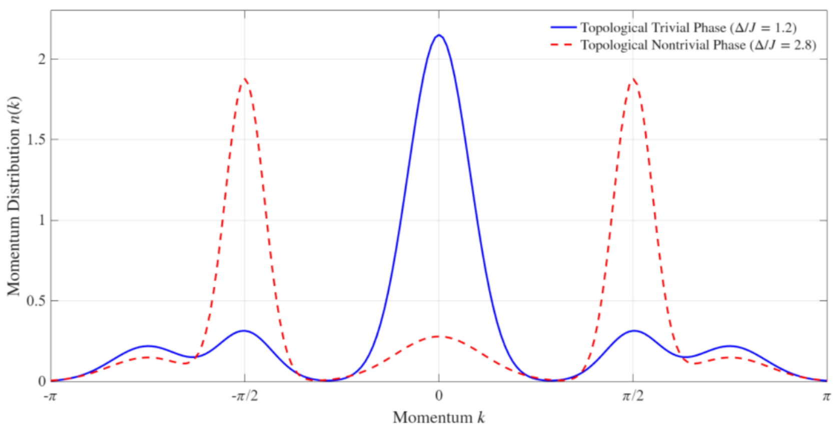

FIGURE 4. Momentum distribution of the topological imprint in momentum space

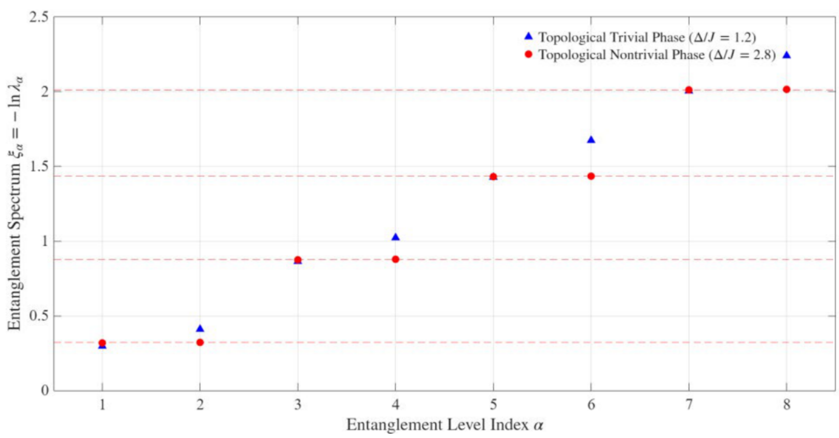

FIGURE 5. Topological degeneracy characteristics of symmetry protection in entanglement spectrum

0.323, and the third and fourth energy levels are 0.876 and 0.879, with the difference between each pair of energy levels being less than 0.003, the spacing between adjacent energy level pairs is approximately 0.55, and the degeneracy is five orders of magnitude higher than the numerical truncation error (10^{-8}). Furthermore, it has converged at a system size of L=60; while in the trivial phase (Δ/J=1.2), there is a significant split of 0.114 between the lowest energy level 0.298 and the second energy level 0.412. This degeneracy stems from the topological protection of the system under

U(1) particle number conservation and spatial reflection symmetry. When the manybody Zak phase $\gamma=\pi$, the ground state has equivalent fractional excitations at the subsystem boundary, resulting in an approximately symmetric doubly degenerate structure for the entangled Hamiltonian. Interactions maintain this many-body coherence, ensuring the degeneracy remains clear in strongly correlated regions. The results show that the doubly degeneracy of the entanglement spectrum is a robust many-body characteristic of topological order in interacting quasi-periodic systems.

IV. CONCLUSION

By constructing a many-body Zak phase theory framework based on quasi-momentum manifolds and utilizing DMRG high-precision ground state solutions, this paper achieves a rigorous characterization of topological phase transitions in interacting Bose-Einstein condensates that provides fundamental insights for engineering the structural topology. This method does not rely on single-particle band structures or bulk gaps and directly extracts topological invariants from the multi-body wavefunction. The data results show that the system is in a stable topologically nontrivial phase at U/J=3.2 and Δ/J=2.8, with a total occupancy rate of nearly 90% within the five edge lattice points. The momentum distribution exhibits a symmetric peak of height 1.87 at $k=\pm\pi/2$, and the entanglement spectrum displays a double degenerate structure with an energy level difference of less than 0.003. These multidimensional indices consistently confirm that interactions and quasi-periodicity can cooperatively stabilize nontrivial topological order. This method provides a computable and verifiable topo-logical classification paradigm for strongly correlated aperiodic quantum systems, offering direct experi-mental feasibility in cold atom quantum simulations.

AUTHOR CONTRIBUTIONS

Jianrong Wen designed, collected and analyzed the data, and drafted the manuscript. Jianrong Wen conducted the study, critically revised the manuscript for important intellectual content, and gave final approval of the version to be published. Jianrong Wen participated fully in the work, take public responsibility for appropriate portions of the content, and agreed to be accountable for all aspects of the work in ensuring that questions related to the accuracy or integrity of any part of the work are appropriately investigated and resolved.

CONFLICTS OF INTEREST

The author declares no conflict of interest.

FUNDING

This research received no external funding.

ACKNOWLEDGEMENTS

Not applicable.

REFERENCES

[1] K. X. Yao, Z. Zhang, and C. Chin, "Domain-wall dynamics in Bose–Einstein condensates with synthetic gauge fields," Nature, vol. 602, no. 7895, pp. 68-72, 2022, doi: 10.1038/s41586-021-04250-3.
[2] C. H. Li, Y. Yan, S. W. Feng, S. Choudhury, D. B. Blasing, and Q. Zhou, "Bose-Einstein condensate on a synthetic topological Hall cylinder," PRX Quantum, vol. 3, no. 1, Art. no. 010316, 2022, doi: 10.1103/PRXQuantum.3.010316.
[3] S. Nakajima, N. Takei, K. Sakuma, Y. Kuno, P. Marra, and Y. Takahashi, "Competition and interplay between topology and quasi-periodic disorder in Thouless pumping of ultracold atoms," Nature Physics, vol. 17, no. 7, pp. 844-849, 2021, doi: 10.1038/s41567-021-01229-9.
[4] K. Roy, S. Roy, and S. Basu, "Quasiperiodic disorder induced critical phases in a periodically driven dimerized pwave Kitaev chain," Scientific Reports, vol. 14, no. 1, Art. no. 20603, 2024, doi: 10.1038/s41598-024-70995-2.
[5] M. Koshino and H. Oka, "Topological invariants in two-dimensional quasicrystals," Physical Review Research, vol. 4, no. 1, Art. no. 013028, 2022, doi: 10.1103/PhysRevResearch.4.013028.
[6] S. N. Nabi, S. Roy, and S. Basu, "Phase properties of interacting bosons in presence of quasiperiodic and random potential," Annals of Physics, vol. 448, no. 1, pp. 169-171, 2023, doi: 10.1016/j.aop.2022.169171.
[7] B. Michen and J. C. Budich, "Nonlinear interference challenging topological protection of chiral edge states," Physical Review A, vol. 108, no. 2, Art. no. L021501, 2023, doi: 10.1103/PhysRevA.108.L021501.
[8] J. Wang, P. Hannaford, and B. J. Dalton, "Many-body effects and quantum fluctuations for discrete time crystals in Bose–Einstein condensates," New Journal of Physics, vol. 23, no. 6, Art. no. 063012, 2021, doi: 10.1088/1367-2630/abea45.
[9] Y. C. Zhang, "Critical regions in a one-dimensional flat band lattice with a quasi-periodic potential," Scientific Reports, vol. 14, no. 1, pp. 1-13, 2024, doi: 10.1038/s41598-024-68851-4.
[10] P. Molignini and B. Chakrabarti, "Stability of dipolar bosons in a quasiperiodic potential," Physical Review Research, vol. 7, no. 2, Art. no. 023237, 2025, doi: 10.1103/PhysRevResearch.7.023237.
[11] Y. Takahashi, "Quantum simulation of quantum many-body systems with ultracold two-electron atoms in an optical lattice," Proceedings of the Japan Academy. Series B, vol. 98, no. 4, pp. 141-160, 2022, doi: 10.2183/pjab.98.010.
[12] B. Hetényi and I. Balogh, "Numerical study of the localization transition of Aubry-André type models," Physical Review B, vol. 112, no. 14, Art. no. 144203, 2025, doi: 10.1103/g7vd-hgw4.
[13] R. Citro and M. Aidelsburger, "Thouless pumping and topology," Nature Reviews Physics, vol. 5, no. 2, pp. 87-101, 2023, doi: 10.1038/s42254-022-00545-0.
[14] M. Ajmal, J. Muhammad, U. Younas, E. Hussian, M. E. Meligy, and M. Sharaf, "Exploring the Gross-Pitaevskii model in Bose-Einstein condensates and communication systems: Features of solitary waves and dynamical analysis," International Journal of Theoretical Physics, vol. 64, no. 3, pp. 1-26, 2025, doi: 10.1007/s10773-025-05937-3.
[15] E. Pavlyshynets, L. Salasnich, B. A. Malomed, and A. Yakimenko, "Solitons in quasiperiodic lattices with fractional diffraction," Physical Review E, vol. 111, no. 4, Art. no. 044206, 2025, doi: 10.1103/PhysRevE.111.044206.
[16] P. P. Gaude, A. Das, and R. V. Pai, "Cluster mean field plus density matrix renormalization theory for the Bose Hubbard models," Journal of Physics A: Mathematical and Theoretical, vol. 55, no. 26, Art. no. 265004, 2022, doi: 10.1088/1751-8121/ac71e7.
[17] E. Akaturk and I. Hen, "Quantum Monte Carlo algorithm for Bose-Hubbard models on arbitrary graphs," Physical Review B, vol. 109, no. 13, Art. no. 134519, 2024, doi: 10.1103/PhysRevB.109.134519.
[18] R. Resta, "The single-point Berry phase in condensed-matter physics," Journal of Physics A: Mathematical and Theoretical, vol. 55, no. 49, Art. no. 491001, 2022, doi: 10.1088/1751-8121/aca84b.
[19] H. Koizumi and A. Ishikawa, "Berry connection from many-body wave functions and superconductivity: Calculations by the particle number conserving Bogoliubov-de Gennes equations," Journal of Superconductivity and Novel Magnetism, vol. 34, no. 11, pp. 2795-2808, 2021, doi: 10.1007/s10948-021-05991-y.
[20] T. Chanda, L. Barbiero, M. Lewenstein, M. J. Mark, and J. Zakrzewski, "Recent progress on quantum simulations of non-standard Bose-Hubbard models," Reports on Progress in Physics, vol. 88, no. 4, Art. no. 044501, 2025, doi: 10.1088/1361-6633/adc3a7.

[21] E. Gottlob and U. Schneider, "Hubbard models for quasicrystalline potentials," Physical Review B, vol. 107, no. 14, Art. no. 144202, 2023, doi: 10.1103/PhysRevB.107.144202.

[22] R. Modak and D. Rakshit, "Many-body dynamical phase transition in a quasiperiodic potential," Physical Review B, vol. 103, no. 22, Art. no. 224310, 2021, doi: 10.1103/PhysRevB.103.224310.

[23] E. Petrova, M. Ljubotina, G. Yalnız, and M. Serbyn, "Finding periodic orbits in projected quantum many-body dynamics," PRX Quantum, vol. 6, no. 4, Art. no. 040333, 2025, doi: 10.1103/tldp-kvkd.

[24] K. Chen, M. Weiner, M. Li, X. Ni, A. Alù, and A. B. Khanikaev, "Nonlocal topological insulators: Deterministic aperiodic arrays supporting localized topological states protected by nonlocal symmetries," Proceedings of the National Academy of Sciences, vol. 118, no. 34, Art. no. e2100691118, 2021, doi: 10.1073/pnas.2100691118.

[25] X. Lin, X. Chen, G. C. Guo, and M. Gong, "General approach to the critical phase with coupled quasiperiodic chains," Physical Review B, vol. 108, no. 17, pp. 22, 2023, doi: 10.1103/PhysRevB.108.174206.

[26] Y. Wang, J. H. Zhang, Y. Li, J. Wu, W. Liu, F. Mei, et al., "Observation of interaction-induced mobility edge in an atomic Aubry-André wire," Physical Review Letters, vol. 129, no. 10, Art. no. 103401, 2022, doi: 10.1103/PhysRevLett.129.103401.

[27] C. Gross and W. S. Bakr, "Quantum gas microscopy for single atom and spin detection," Nature Physics, vol. 17, no. 12, pp. 1316-1323, 2021, doi: 10.1038/s41567-021-01370-5.

[28] D. Hannukainen J, F. Martínez M, H. Bardarson J, and T. K. Kvorning, "Interacting local topological markers: A oneparticle density matrix approach for characterizing the topology of interacting and disordered states," Physical Review Research, vol. 6, no. 3, Art. no. L032045, 2024, doi: 10.1103/PhysRevResearch.6.L032045.

[29] K. Sarkar S, T. Mishra, P. Muruganandam, and P. K. Mishra, "Quench-induced chaotic dynamics of Anderson-localized interacting Bose-Einstein condensates in one dimension," Physical Review A, vol. 107, no. 5, Art. no. 053320, 2023, doi: 10.1103/PhysRevA.107.053320.